Molecular Biology of the Cell
Vol. 6, 661–674, June 1995

Specialized Functional Properties of the Integrin α^4 Cytoplasmic Domain

Paul D. Kassner,* Ronen Alon,† Timothy A. Springer,† and Martin E. Hemler*‡

*Dana-Farber Cancer Institute, and †The Center for Blood Research, Harvard Medical School, Boston, Massachusetts 02115

Submitted February 9, 1995; Accepted March 24, 1995
Monitoring Editor: Masatoshi Takeichi

For functional studies of the integrin α^4 cytoplasmic domain, we have expressed the following in K562 and Chinese hamster ovary (CHO) cells: 1) wild-type α^4 (called X4C4), 2) two chimeric forms of α^4 (called X4C2 and X4C5) that contain the cytoplasmic domains of α^2 and α^5, respectively, and 3) α^4 with no cytoplasmic domain (X4C0). Cytoplasmic domain exchange had no effect on VLA-4–dependent static cell adhesion or tethering to VCAM-1 in conditions of shear flow. However, the presence of the α^2 or α^5 tails markedly enhanced VLA-4–dependent K562 cells spreading (X4C2 > X4C5 > X4C4 > X4C0), increased localization of VLA-4 into focal adhesion-like complexes in CHO cells (X4C2 > X4C5 > X4C4), and strengthened CHO and K562 cell resistance to detachment from VCAM-1 in conditions of shear flow (X4C2 > X4C5 > X4C4 > X4C0). Conversely, the α^4 tail supported greater VLA-4–dependent haptotactic and chemotactic cell migration. In the absence of any α tail (i.e., X4C0), robust focal adhesions were observed, even though cell spreading and adhesion strengthening were minimal. Thus, such focal adhesions may have relatively little functional importance, and should not be compared with focal adhesions formed when α tails are present. Together, these results indicate that all three α-chain tails exert defined positive effects (compared with no tail at all), but suggest that the α^4 cytoplasmic domain may be specialized to engage in weaker cytoskeletal interactions, leading to diminished focal adhesion formation, cell spreading, and adhesion strengthening, while augmenting cell migration and facilitating rolling under shear flow. These properties of the α^4 tail are consistent with the role of α^4 integrins on highly motile lymphocytes, monocytes, and eosinophils.

INTRODUCTION

The α^4 integrins ($\alpha^4\beta_1$ and $\alpha^4\beta_7$) facilitate the in vivo recruitment of lymphocytes, monocytes, and eosinophils to sites of inflammation in various disease models (Lobb and Hemler, 1994). Also, α^4 integrins play important roles in myogenesis (Rosen *et al.*, 1992), melanoma metastasis (Qian *et al.*, 1994), and hematopoiesis (Williams *et al.*, 1991; Papayannopoulou and Nakamoto, 1993). Ligands for $\alpha^4\beta_1$ (also called VLA-4) include the VCAM-1 molecule expressed on activated endothelial cells and other cell types (Elices *et al.*, 1990; Rice *et al.*, 1990; Schwartz *et al.*, 1990), and the alternatively spliced CS1 region of fibronectin (García-Pardo and Ferreira, 1989; Elices *et al.*, 1990; Guan and Hynes, 1990; Wayner *et al.*, 1989). The $\alpha^4\beta_7$ integrin binds to MadCAM, and thus mediates lymphocyte homing to intestinal tissue (Berlin *et al.*, 1993). Like $\alpha^4\beta_1$, $\alpha^4\beta_7$ can also mediate cell attachment to VCAM-1 and to the CS1 region of fibronectin (Chan *et al.*, 1992a; Rüegg *et al.*, 1992). The $\alpha^4\beta_1$ and $\alpha^4\beta_7$ integrins are primarily expressed on various leukocytes, although α^4 integrins may also appear on some nonhematopoietic tumor cells (Rice and Bevilacqua, 1989), and in vascular smooth muscle, skeletal muscle, and a number of other tissues in the developing embryo (Sheppard *et al.*, 1994; Stepp *et al.*, 1994). Mouse embryos lacking α^4 failed to undergo fusion of the allantois with the chorion during placentation, and also failed to develop

‡ Corresponding author: Dana-Farber Cancer Institute, Rm M613, 44 Binney St., Boston, MA 02115.

epicardium and coronary vessels (Yang *et al.*, 1995), thus proving conclusively the in vivo relevance of α^4 integrins.

Adhesion mediated by $\alpha^4\beta_1$ may promote (Damle *et al.*, 1993) or inhibit (Koopman *et al.*, 1994) cell death, and also may trigger "outside-in" signaling events including tyrosine phosphorylation of a 105-kDa protein in lymphocytes (Nojima *et al.*, 1992; Freedman *et al.*, 1993), the production of inflammatory mediators (Yurochko *et al.*, 1992), and the synthesis of 72-kDa gelatinase (Romanic and Madri, 1994). Furthermore, VLA-4 interaction with ligand can lead to cell migration through endothelium (Chuluyan and Issekutz, 1993), through coated filters (Chan and Aruffo, 1993), and through stromal cell layers (Miyake *et al.*, 1992). Notably, VLA-4 can also mediate leukocyte tethering to VCAM-1 in conditions of shear flow, followed by rolling and stable adhesion (Alon *et al.*, 1995).

The cytoplasmic domains of integrins play critical roles in regulating both ligand binding "inside-out" signaling (O'Toole *et al.*, 1991, 1994) and post-ligand binding outside-in signaling events (Sastry and Horwitz, 1993; Hemler *et al.*, 1994). For example, the organization of focal adhesion complexes (Burridge *et al.*, 1988) depends on integrin β-chain tails (Marcantonio *et al.*, 1990; LaFlamme *et al.*, 1992; Reszka *et al.*, 1992) and is negatively regulated by α-chain tails (Briesewitz *et al.*, 1993; Ylänne *et al.*, 1993; Kawaguchi *et al.*, 1994). Also, single chain β_1 tail chimeras can exert dominant negative effects on several integrin functions, presumably by disrupting critical cytoskeletal associations (Chen *et al.*, 1994; LaFlamme *et al.*, 1994; Lukashev *et al.*, 1994; Smilenov *et al.*, 1994). In a study involving an integrin β_1 cytoplasmic domain chimera, the ability to organize focal adhesions in Chinese hamster ovary (CHO) cells was correlated positively with cell proliferation, and negatively with cell migration (Pasqualini and Hemler, 1994).

Previously, cytoplasmic domain chimeras were used to show that the integrin α^4 cytoplasmic domain was better able to support VLA-2–mediated random cell migration, but contributed minimally toward VLA-2–mediated collagen gel contraction (Chan *et al.*, 1992b). In this study, cytoplasmic domain chimeras are again utilized, but now the α^4 tail is analyzed in its most relevant context, i.e., within the VLA-4 molecule itself. Chimeric α^4 chains have been expressed both in CHO cells where VLA-4 is constitutively very active (Kassner *et al.*, 1994), and in K562 cells where it is relatively inactive (Kassner and Hemler, 1993). Using these cells under conditions of shear flow, we uncovered important adhesion strengthening differences between integrin cytoplasmic domains, not previously discernable in static adhesion assays. Also we have made the novel observation that α-chain tails can differentially affect cell spreading and focal adhesion formation.

MATERIALS AND METHODS

Antibodies and Purified Ligands

Antibodies used were mouse anti-human α^4, B-5G10 (Hemler *et al.*, 1987), and HP1/2 (Sánchez-Madrid *et al.*, 1986); mouse negative control antibody J2A2 (Hemler and Strominger, 1982); rabbit antisera against phosphotyrosine (purchased from Transduction Laboratories, Lexington, KY); fluorescein isothiocyanate- or rhodamine-conjugated goat anti-mouse antisera (Calbiochem, La Jolla CA); and rhodamine-conjugated goat anti-rabbit antisera (Calbiochem). Whole fibronectin and the 40-kDa chymotryptic fragment of fibronectin (FN40), which contains the CS1 region, were purified as described (Garcia-Pardo *et al.*, 1987). Recombinant soluble VCAM-1 (sVCAM-1) containing seven Ig domains was previously described (Lobb *et al.*, 1991).

Constructs, Transfection, and Cell Culture

The chimeric and truncated α^4 cDNAs, K562 transfectants, and CHO-Neo, -X4C0, -X4C2, -X4C4, and -X4C5 transfectants were prepared as previously described (Kassner and Hemler, 1993; Kassner *et al.*, 1994). The K562 transfectants were maintained in RPMI 1640 medium, and CHO transfectants were maintained in MEM α medium (without ribonucleosides or deoxyribonucleosides). Both media also contained 10% fetal bovine serum (FBS), 10 mM *N*-2-hydroxyethylpiperazine-*N'*-2-ethanesulfonic acid (HEPES), and 10 mM L-glutamine.

Cell Spreading

Glass coverslips were coated for 2 h at 37°C with FN40 or sVCAM-1 diluted in 0.1 M $NaHCO_3$; nonspecific binding sites were blocked by incubation with 0.1% heat-denatured bovine serum albumin (BSA) in phosphate-buffered saline (PBS) for 1 h. Cells were washed sequentially in PBS containing 0.5 mM EDTA, then in PBS, and resuspended in RPMI 1640 medium containing 0.1% BSA at 10^6 cells/ml. Coverslips were placed in 35-mm petri dishes and covered with 2.0 ml RPMI/0.1%BSA, and then 100 μl of cell suspension was added to the center of the dish and the cultures were incubated at 37°C for 1 h. Unbound cells were removed by washing the coverslips three times with PBS, and cells were fixed with 3% paraformaldehyde for 20 min at room temperature. Coverslips were treated with mounting media (FluorSave, Calbiochem), and then cell spreading, essentially an all or none event, was easily assessed by visual inspection of at least three high power fields, and the percentage of spread cells (relative to the number of attached cells) was calculated. Cell spreading results were also confirmed by quantitative planar morphometry using the Microcomp Image analysis system as described (Byers *et al.*, 1991).

Flow Cytometry and Adhesion Assays

For flow cytometry, 10^6 cells were stained with negative control monoclonal antibody (mAb) or anti-α^4 mAb, followed by FITC-conjugated goat anti-mouse IgG (Calbiochem), and then analyzed using a FACScan machine (Becton Dickinson, Mountainview, CA) as described elsewhere (Elices *et al.*, 1990).

Adhesion assays were essentially as described (Chan *et al.*, 1992a; Kawaguchi and Hemler, 1993). Briefly, cells were labeled with the fluorescent dye BCECF-AM [2',7'-*bis* (2-carboxyethyl)-5(6)-carboxyflorescein] (Molecular Probes, Eugene, OR), and then 5×10^4 cells/well were added to 96-well microtiter plates coated with VCAM-1 or FN40. After 20 min of incubation at 37°C, unbound cells were removed and attached cells were analyzed using the Cytofluor 2300 measurement system (Millipore, Bedford, MA). Background binding (assessed using BSA-coated wells) was typically less than 5% of the total, and is subtracted from the results reported as the mean ± SD of triplicate determinations.

Immunofluorescence Microscopy

Circular glass coverslips (12 mm; Fisher Scientific, Pittsburgh, PA) were spotted with 15 μl of FN40 (50 μg/ml) or vitronectin (10 μg/ml) in PBS, and then allowed to dry overnight at room temperature, before blocking with PBS containing 1% heat-denatured BSA for 1–4 h at 37°C. CHO cells were harvested in PBS containing 2 mM EDTA, pelleted, then resuspended in MEM α medium containing 10 mM HEPES and 1% FCS that had been depleted of fibronectin. Cells were plated onto coverslips and allowed to spread for 2–16 h at 37°C. Cells were then rinsed once in PBS containing 2 mM $MgCl_2$, and fixed and permeabilized in PBS containing 2% paraformaldehyde, 1% NP-40, and 2 mM $MgCl_2$ for 20 min at room temperature. Nonspecific binding sites were blocked with 20% goat serum in PBS for 1 h at room temperature. Primary antibodies (HP1/2, 1:1000 dilution of ascites, or anti-phosphotyrosine, 1:500 dilution of antisera) were diluted in 20% goat serum and incubated with cells for 2 h at room temperature or 16 h at 4°C. Coverslips were washed five times with PBS, before incubation with secondary antibodies (rhodamine-conjugated goat anti-mouse IgG, or rhodamine-conjugated goat anti-rabbit IgG, each at 1:100 in 20% goat serum) for 1 h at room temperature. Finally, coverslips were washed five times with PBS, rinsed once in ddH_2O, mounted on glass slides in FluorSave reagent (Calbiochem), and photographed within 1 wk using a Axioskop fluorescent microscope (Zeiss, Thornwood, NY).

Tethering and Shear Resistance in Flow

Assays were performed essentially as previously described (Lawrence and Springer, 1991; Alon *et al.*, 1995). Briefly, polystyrene dishes were spotted with sVCAM-1 or FN40, quenched with human serum albumin, and these plastic dishes were assembled as the lower wall in a parallel wall flow chamber and mounted on the stage of an inverted phase-contrast microscope. K562 cells (400,000/ml) and CHO cells (200,000/ml) were resuspended in Hanks' balanced salt solution, containing 10 mM HEPES (pH 7.4), 1 mM Mg^{2+}, and 2 mM Ca^{2+}, and then perfused through the flow chamber at different flow rates to obtain the indicated shear stresses at the chamber wall. Tethering was determined by counting (from videotaped images) the cells remaining adherent (either rolling or firmly bound) for at least 3 s in a given field of view (0.43 mm^2) during the first 60 s of continuous shear flow. Complete inhibition by anti-α^4 blocking antibodies, and lack of any interaction with surfaces coated with human serum albumin, confirmed the specificity of tethering. For detachment assays, tethered cells were first allowed to accumulate at low shear flow (0.36 dynes/cm^2) unless otherwise indicated. Then, as shear flow was increased by 2–2.5 fold increments every 10 s, the number of cells remaining bound at each interval was determined.

Migration Assays

Migration assays were carried out in 96-well format chemotaxis chambers using framed polycarbonate filters with 8-μm pores (Neuroprobe, Cabin John, MD). For haptotactic migration assays, filters were spotted with matrix protein diluted in 0.1 M $NaHCO_3$ and allowed to dry. Then 32 μl MEM α medium with 1% FBS (fibronectin depleted) was placed in the lower wells of the 96-well chamber, and filters were rinsed with PBS and inverted (matrix side down) before the chamber was assembled. Cells were harvested using 2 mM EDTA in PBS, labeled with BCECF-AM (5 μg/ml, Molecular Probes) for 30 min, pelleted, and resuspended in MEM α medium with 1% FBS (serum depleted) at a concentration of 5×10^5 cells/ml. Then, 60 μl cell suspension (3×10^4 cells/well) was added to the upper wells, and the chamber was incubated at 37°C for 4 h. For chemotactic migration assays, filters were coated (on both sides) by immersion in matrix protein diluted in 0.1 M $NaHCO_3$ overnight at 4°C, and rinsed in PBS before use. Before assembly of the chamber, 32 μl MEM α medium with 1% FBS (serum depleted) was added to the lower wells. Cells were harvested and labeled as described above, except that before plating, they were resuspended in MEM without serum, and incubated at 37°C for 2 h. After the cells were allowed to migrate (in either the haptotactic or chemotactic assay), media was removed from the upper chambers by inversion, cells attached to the upper side of the filter were mechanically removed by scraping, and cells migrating to the lower side of the filters were quantitated by reading filters in the Cytofluor 2300 fluorescence measurement system (Millipore). The percent of cell migration was calculated from the following: (fluorescence of cells on lower face of filter)/(total fluorescence of input cells) × 100. For blocking studies, cells were incubated with purified HP1/2 (2 g/ml) for 30 min before plating. Results are reported as the mean migration from six replicates ± SD.

RESULTS

Expression of Chimeric α^4 Integrins

For comparative analysis of the α^4 cytoplasmic domain, cDNAs encoding a series of chimeric and truncated forms of α^4 were prepared and expressed in the K562 (erythroleukemic) and CHO cells lines as described previously (Kassner *et al.*, 1994; Kassner and Hemler, 1993). Transfectants expressing similar levels of the unaltered, chimeric, and deleted forms of the α^4 chain were selected by fluorescence-activated cell sorting (FACS). Typical α^4 expression profiles are shown in Figure 1 for the various transfected K562 and CHO cell lines. As previously noted, neither K562 nor CHO cells express any detectable endogenous integrin α^4 or α^2 subunits (Kassner and Hemler, 1993; Kawaguchi and Hemler, 1993; Kassner *et al.*, 1994), but CHO cells do express hamster α^5 (Schreiner *et al.*, 1989).

Cell Adhesion and Spreading Mediated by Mutant α^4 Integrins

Exchange of the α^4 cytoplasmic domain did not alter VLA-4–dependent adhesion. In a standard 20-min static cell adhesion assay, the X4C2, X4C4, and X4C5 molecules supported similar adhesion of K562 cells to either sVCAM-1 or FN40. In contrast, the X4C0 mutant supported diminished adhesion (Figure 2, A and B). The loss of adhesion because of tail deletion was not as great as seen previously (Kassner and Hemler, 1993) because of the high coating concentrations of sVCAM (10 μg/ml) and FN40 (40 μg/ml) used in this experiment.

After the adhesion assay, the assay plate was incubated for an additional 40 min at 37°C, and cell spreading was analyzed. As indicated, the X4C2 and X4C5 mutants supported elevated K562 cell spreading (on either sVCAM-1 or FN40) compared with the X4C4 and X4C0 molecules (Figure 2, C and D). In additional experiments at lower sVCAM coating levels (5 μg/ml), the disparity between X4C2 and X4C5 compared with X4C4 and X4C0 was even more obvious (Figure 2, E and F), as a greater percentage of K562 cells expressing the former showed spreading. The data from multiple VCAM spreading experiments

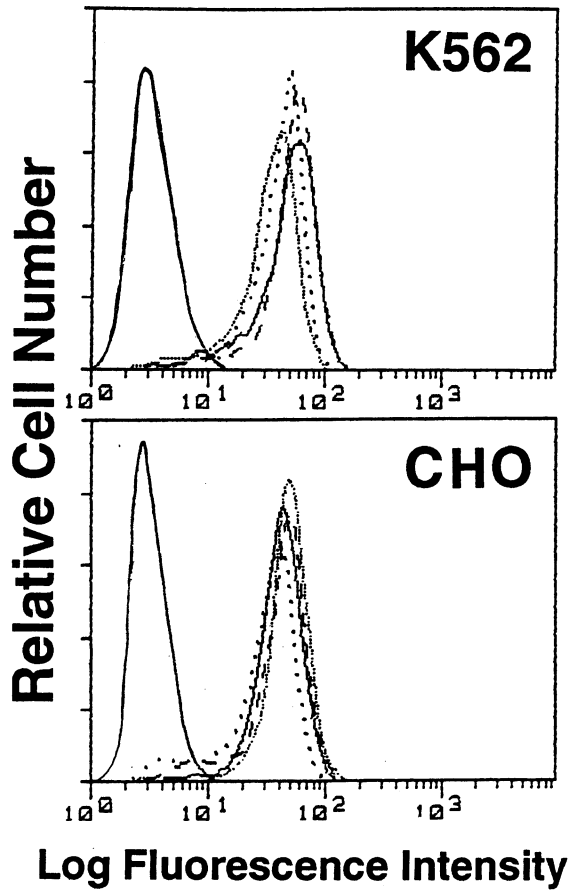

Figure 1. Expression of α^4 mutants in K562 and CHO cell lines. The K562 (upper) and CHO (lower) cells expressing X4C0 (•••••), X4C2 (·····), X4C4 (- - -), and X4C5 (———) protein were stained with the anti-α^4 mAb B-5G10 and analyzed by flow cytometry..Neo control transfectants stained with B-5G10 are indicated by the solid lines shown on the left.

showed that if the X4C2 results were arbitrarily set at 100%, then X4C5 = 64% (n = 5), X4C4 = 13% (n = 7), and X4C0 = 5.7% (n = 5). Whereas the data in Figure 2 were collected after 1 h, similar differences in cell spreading were obvious from 45 min through at least 4 h after cell plating.

Image analysis of total bound cells (including both spread and unspread) on sVCAM-1 confirmed the results from visual inspection. Precise measurements of cell symmetry and angularity (Byers *et al.*, 1991) showed that X4C2 and X4C5 transfectants had a mean cellular geometry significantly different from the X4C4-K562 cells ($p < 0.001$). A photograph of α^4-transfected K562 cells bound to sVCAM-1 further emphasizes that, even without image analysis, bound cells expressing X4C2 and X4C5 show obviously greater spreading than bound cells expressing X4C4 or X4C0 (Figure 3). In a control experiment, K562 cells transfected with pFNeo vector alone showed no binding or spreading on sVCAM-1. CHO cell transfectants were not used in VLA-4–dependent spreading assays because of their high level of background spreading.

Localization of α^4 Integrins into Focal Adhesion Complexes

Despite many attempts, utilizing several different cell lines, we consistently failed to observe the localization of α^4 integrin into focal adhesion-like complexes. This was true even in CHO cells, where we previously observed conspicuous β_1, α^5, and α^2 localization into focal adhesions (Kawaguchi *et al.*, 1994; Pasqualini and Hemler, 1994). For example, CHO cells containing unaltered α^4 (X4C4) spread very well on surfaces coated with FN40 protein, but showed a mixture of diffuse and punctate α^4 staining, with few focal adhesion-like structures (Figure 4, B and F). However, us-

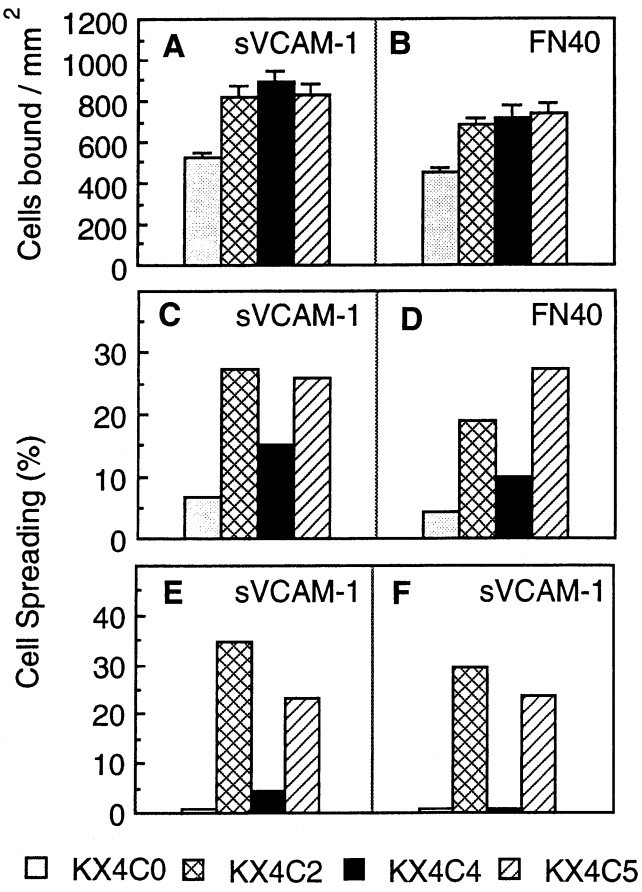

Figure 2. Adhesion and cell spreading of K562 transfectants on sVCAM-1 and FN40. Adhesion assays (A and B) were done concurrently with cell spreading assay (C and D) as described in MATERIALS AND METHODS and text. Plates were coated with 10 μg/ml sVCAM-1 (A and C) or 40 μg/ml FN40 (B and D). Two additional cell spreading assays were done on coverslips coated with 5 μg/ml sVCAM-1 (E and F). For these assays, errors (SD) ranged from 1.5–4.5% of total cells, and were typically less than 2.5%.

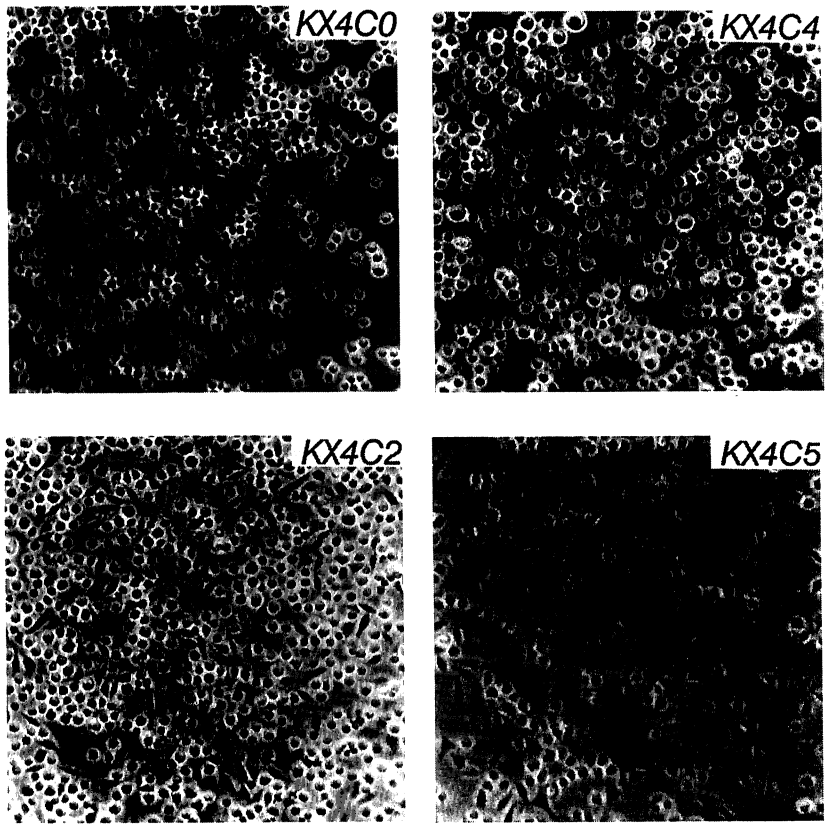

Figure 3. Cell spreading of K562 transfectants on sVCAM-1. Coverslips were coated with sVCAM-1 (10 g/ml) then blocked with 0.1% BSA. Transfectants were plated in RPMI medium with 0.1% BSA and allowed to attach and spread for 1 h at 37°C. Unbound cells were removed by rinsing three times with PBS, and then the remaining cells were fixed with 3% paraformaldehyde and photographed.

ing the same conditions, we clearly observed localization of the X4C5 (Figure 4, C and G) and X4C2 (Figure 4, A and E) proteins into focal adhesion-like complexes within CHO cells. Furthermore, at all time points examined between 2 and 16 h, the CHO-X4C2 cell line, followed by CHO-X4C5, showed substantially more focal adhesion complexes than CHO-X4C4. For example, after spreading on FN40 for 4 h, the visually estimated percentages of cells showing α^4 in focal adhesions were 79 and 10 for X4C2-, and X4C4-CHO cells, respectively. After 7 h, the percentages were 93, 28, and 79 for X4C2-, X4C4-, and X4C5-CHO cells, respectively (Table 1). Together these results provide compelling evidence that the α^4 tail, in contrast to the α^5 and α^2 tails, may selectively impede α^4 integrin localization into focal adhesions. Similar results were obtained when intact fibronectin was utilized (Kassner, unpublished data).

Notably, CHO cells expressing the α^4 tail-deletion mutant (X4C0) were readily able to initiate ligand-dependent formation of focal adhesions (Figure 4, D and H), comparable to those seen with X4C2 (Figure 4, A and E, and see also the numbers in Table 1). This result confirms that the extracellular and transmembrane regions of α^4 are not intrinsically deficient in ability to localize into focal adhesions. In contrast to the results obtained using FN-40 (Figure 4), no consistent formation of focal adhesion-like structures was seen for any of the cells attached to surfaces coated with VCAM-1 or CS1 peptide. Presumably focal adhesion formation is impaired because these substrates fail to provide an essential heparin binding capability that is present within intact fibronectin and the FN40 fragment (Woods *et al.*, 1993). A control experiment (Figure 5A) showed only background staining of mock-transfected CHO cells by anti-α^4 mAb. Additional control experiments showed that within CHO cells spread on vitronectin, neither X4C4, X4C5, nor X4C2 localized into focal adhesions, as expected because vitronectin is not a ligand for α^4 integrins. Nonetheless, within the X4C2-, X4C4-, and X4C5-CHO transfectants, phosphotyrosine staining revealed prominent focal adhesions (Figure 5, B, C, and D), whose formation was most likely initiated by α^V integrin(s). Thus, there is no inherent deficiency in the focal adhesion forming machinery in any of these cell lines.

Tethering under Flow Conditions

We recently showed that the $\alpha^4\beta_1$ integrin, under flow conditions, is capable of mediating tethering to sVCAM-1, followed by rolling adhesions, and then firm attachment (Alon *et al.*, 1995). To compare the

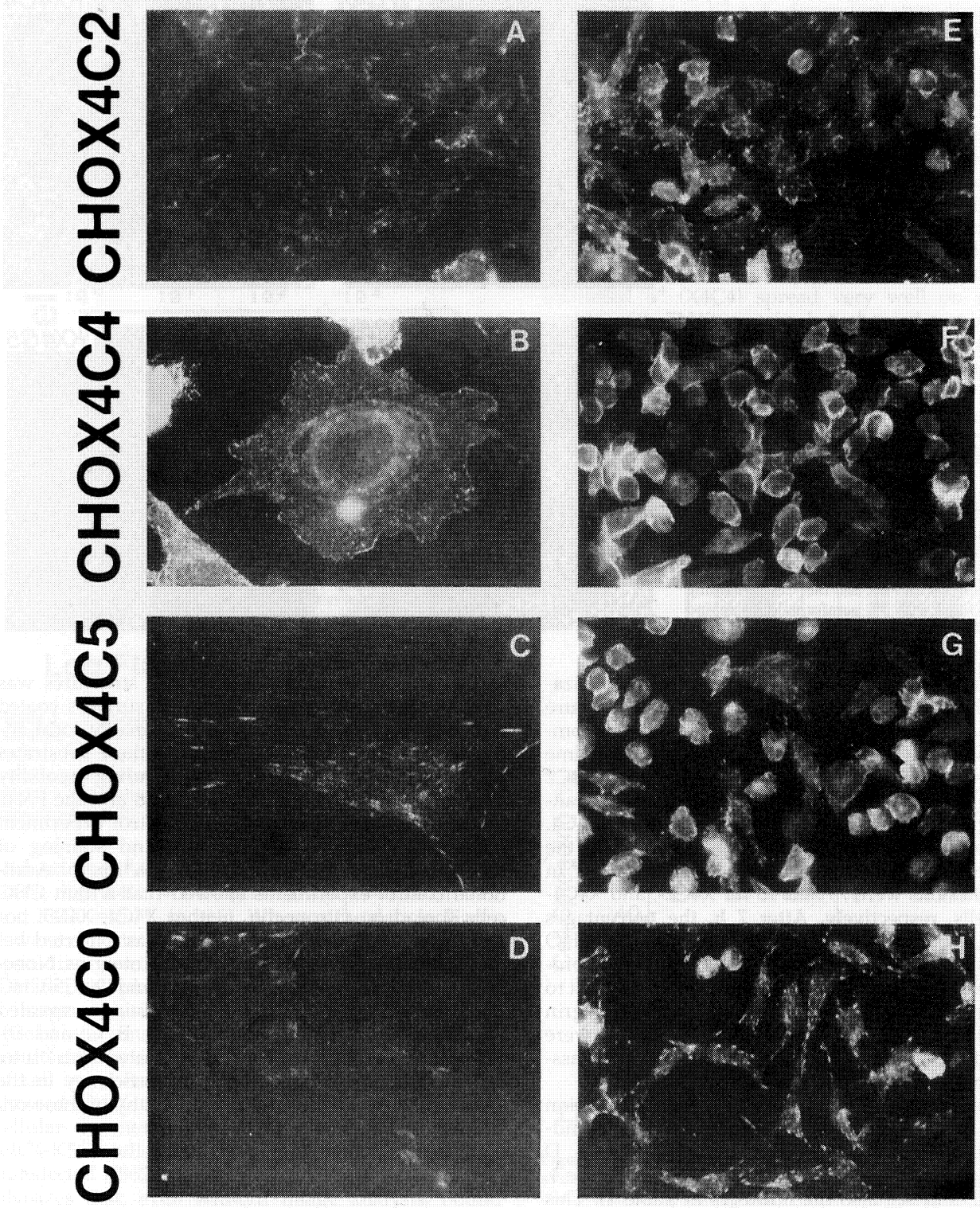

Figure 4. Immunofluorescent localization of α^4 chimeric molecules within CHO cells. CHO-X4C2 (A and E), -X4C4 (B and F), -X4C5 (C and G), and -X4C0 (D and H) transfectants were plated on FN40 (50 μg/ml) for 4 h before fixation and staining with anti-α^4 mAb HP1/2 as described in MATERIALS AND METHODS.

Table 1. Comparison of α^4 mutant localization into focal adhesions

Mutant	Estimated % focal adhesions[a]	
	4 h	7 h
X4C0	86 ± 5 (5)	84 ± 3 (4)
X4C2	79 ± 8 (3)	93 ± 2 (2)
X4C4	10 ± 7 (5)	28 ± 16 (4)
X4C5	...	79 ± 9 (4)

[a] Cells were seeded onto coverslips coated with 50 μg/ml FN40, then allowed to spread for 4 or 7 h. Cells were stained with both anti-α^4 MAb and the percent of cells with α^4 in focal adhesions was visually estimated as described in MATERIALS AND METHODS, and is presented as the mean ± SD of (N) independent coverslips analyzed.

contributions of distinct α-chain cytoplasmic domains to cell tethering, our various K562 and CHO transfectants were perfused into a flow chamber at different wall shear stresses, and then tethering to sVCAM-1 was monitored. As indicated (Figure 6), there was no consistent difference in tethering efficiency among the X4C0-, X4C2-, X4C4- and X4C5-transfectants, regardless of the wall shear stress, VCAM-1 density, or cell type utilized. Thus, the initial cell attachment to sVCAM-1 in flow (i.e., tethering) is not markedly affected by the identity of the α-chain cytoplasmic tail, and in fact does not even require an α cytoplasmic tail, consistent with previous results (Alon *et al.*, 1995). Notably, the overall tethering efficiency was elevated at the lower shear stress (compare 0.73 and 0.36 dynes/cm^2, Figure 6, A and B), and decreased at a lower VCAM-1 density (compare 20 and 1 μg, Figure 6, B and C). Also, α^4-dependent tethering of CHO cells was more efficient than tethering of K562 cells, resulting in similar tethering levels in Figure 6, A and B, even though the VCAM-1 density was 10-fold lower

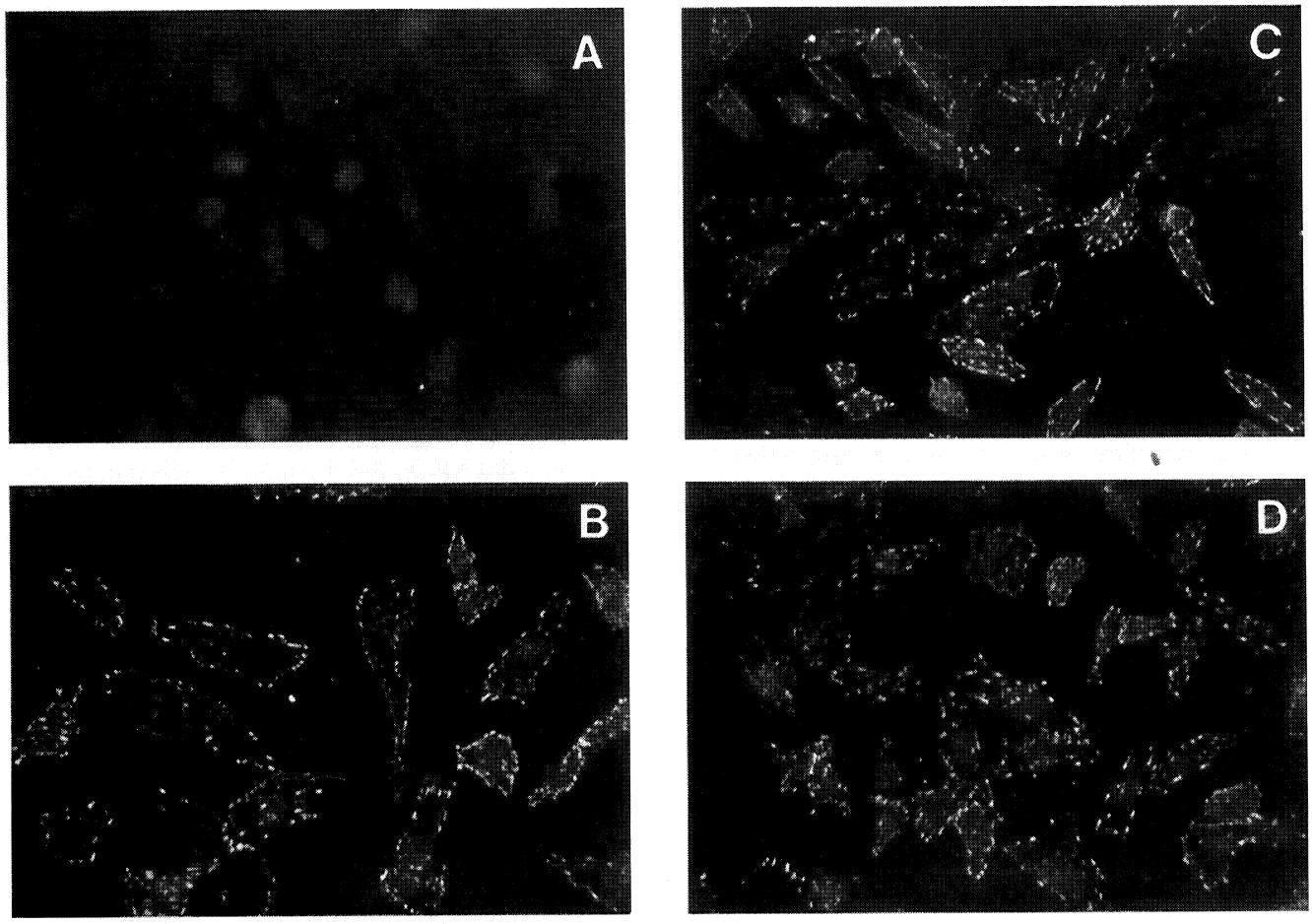

Figure 5. Control experiments for focal adhesions in CHO transfectants. (A) CHO-Neo cells were plated on FN40 (50 g/ml) for 4 h before fixation, and then stained with the anti-α^4 mAb HP1/2. Also, CHO-X4C2 (B), -X4C4 (C), and -X4C5 (D) cells were plated on vitronectin (10 g/ml) for 4 h before fixation and staining with anti-phosphotyrosine antisera as described in MATERIALS AND METHODS.

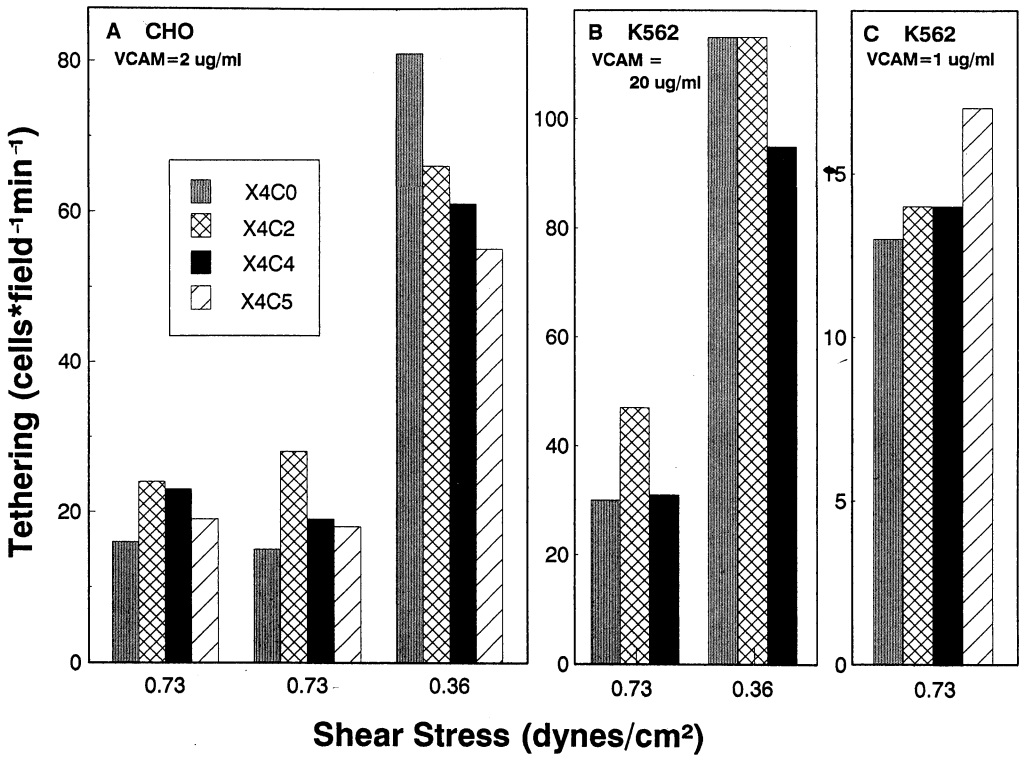

Figure 6. Tethering of CHO and K562 transfectants on sVCAM-1. (A) CHO transfectants were perfused into the flow chamber at either 0.73 dynes/cm^2 or 0.36 dynes/cm^2 of wall shear stress for 60 s, and tethering to sVCAM-1 (2 μg/ml) was analyzed as described in MATERIALS AND METHODS. All cells remained stationary upon tethering. Experiments are representative of three independent assays. (B) K562 cells were perfused into the chamber at either 0.73 or 0.36 dynes/cm^2, and tethering to sVCAM-1 (20 μg/ml) was monitored for 60 s. (C) K562 transfectants were perfused into the flow chamber at a wall shear stress of 0.73 dynes/cm^2, and tethering to low density sVCAM-1 (1 μg/ml) was monitored for 60 s. For parts B and C, cells were considered "tethered" if they remained adherent (either rolling or stationary) for at least 3 s.

for CHO cells than K562 transfectants. This result is consistent with previous observations that VLA-4–dependent adhesion is more avid in CHO cells than in K562 cells (Kassner and Hemler, 1993; Kassner *et al.*, 1994).

Resistance to Shear Stress

Although not playing a major role during tethering, the α^4 cytoplasmic domain does contribute to adhesion strengthening, measured as resistance to detachment under shear (Alon *et al.*, 1995). Consistent with its high constitutive activity in CHO cells (Kassner *et al.*, 1994), VLA-4 mediated tethering under shear flow that was followed by spontaneous arrest (Alon *et al.*, 1995), but not rolling.

To compare the contributions of distinct α-chain cytoplasmic domains to adhesion strengthening under flow conditions, we first allowed CHO cells in low flow (i.e., 0.36 dynes/cm^2) to attach to a low density of sVCAM-1. Then, as the shear stress was incrementally elevated up to 35 dynes/cm^2, the X4C2 and X4C5 cells clearly showed more resistance to detachment than did the X4C4 and X4C0 cells (Figure 7A). For example, at a shear force of 14 dynes/cm^2, 82% of X4C2-CHO and 57% of X4C5-CHO cells resisted detachment, whereas only 24% of X4C4-CHO and 2% of X4C0-CHO cells remained attached.

In another experiment, FN40 was utilized instead of VCAM-1. To overcome a poor tethering efficiency, cells were allowed to tether in very low shear (0.14 dynes/cm^2) to a surface coated with a high density of FN40 (40 μg/ml). Nonetheless, after 3 min, each CHO transfectant showed comparable tethering. Then, as the shear stress was incrementally elevated, the X4C2-cells clearly showed much more resistance to detachment than did X4C5-, X4C4-, or X4C0-cells (Figure 7B). At the highest shear stresses, the X4C0-cells were most readily detached.

Previously we saw that, in contrast to CHO cells, K562 cell tethering on VCAM-1 was followed by rolling, but not firm arrest unless the VLA-4 integrin was activated with manganese or anti-β_1 antibody (Alon *et al.*, 1995). As shown here in Figure 8A, K562-X4C0 cells were most easily detached from high density VCAM by increasing shear forces, followed by X4C4-, and then X4C2-cells. At shear stresses below 10 dynes/cm^2, differences between the numbers of X4C4- and X4C2-cells that remained bound (both rolling plus stationary) were not obvious. However, at these low shear stresses (e.g., at 3.6 dynes/cm^2), high proportions of the bound X4C4-K562 (75%) and X4C0-K562 (80%) were rolling, whereas only 18% of the bound X4C2-K562 cells rolled (Figure 8B). Thus, the α^2 tail can suppress rolling and yield firm arrest even in the

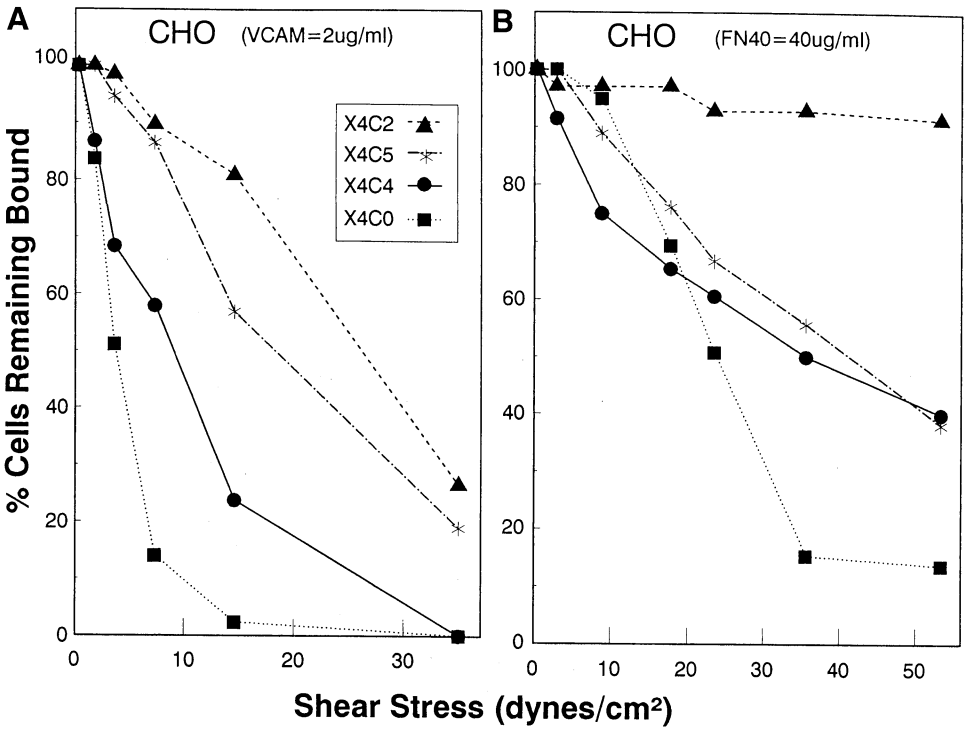

Figure 7. Resistance to shear stress by CHO transfectants on sVCAM-1. (A) After attachment of CHO cells to sVCAM-1 (2 μg/ml), under a shear flow of 0.73 dynes/cm^2 for 30 s, the wall shear stress was incrementally increased (as in Figure 7), and the percentage of cells remaining bound was determined at each step. (B) CHO cells were allowed to attach to FN40 (40 μg/ml) and accumulate for 3 min at a very low shear flow (0.14 dynes/cm^2). Then shear stress was increased (as above) and the percentage of cells remaining bound after each interval was determined. At least 40–70 cells were analyzed in each detachment experiment. Results are representative of three independent experiments.

absence of activation with manganese or anti-β_1 antibody.

At low VCAM density (1 μg/ml), fewer K562 cells attached, and those that had attached were readily detached by increasing shear, with minimal rolling. Nonetheless, when shear stress was increased incrementally up to 3.6 dynes/cm^2, monitoring of cell detachment revealed that the X4C0- and X4C4-transfectants were entirely detached (Figure 8C). In contrast, substantial numbers of X4C2 and X4C5 transfectants remained attached (20 and 10%, respectively).

Cell Migration Mediated by α^4 Chimeras

Previous results had shown an association between the α^4 cytoplasmic domain and increased random cell migration (Chan *et al.*, 1992b). Here we have utilized a different integrin, a different ligand, another cell type, and different migration assays to confirm that the α^4 tail can support elevated cell migration. For chemotactic migration assays, cells were plated on the upper side of porous filters (previously coated on both sides with FN40), and then allowed to migrate toward the 1% FBS present in the lower chamber. In seven representative experiments (Figure 9, A and B), the CHO-X4C4 transfectant showed the highest level of migration, the CHO-X4C5 and -X4C2 cells exhibited markedly less migration than -X4C4, and the -X4C0 cells showed only background migration (comparable with neo-transfected CHO cells). This chemotactic migration through FN40-coated filters was predominantly α^4-dependent as indicated by the low migration of the CHO-Neo transfectants, and the substantial inhibition of migration (60–80%) by the α^4-blocking mAb HP1/2. Each of the transfectants showed similar chemotactic migration through porous filters coated with vitronectin, indicating that there was no essential difference in the non-α^4–dependent migratory capacity of the cells.

For haptotactic migration assays, cells were plated on the upper side of a porous filter, and allowed to migrate toward FN40 that had been coated on the underside of the filter. In seven representative experiments, CHO-X4C4 cells again showed substantially greater migration than -X4C0, X4C2, or -X4C5 transfectants (Figure 9, C and D). By the same criteria mentioned above, this migration was predominantly α^4-dependent. Also, our unpublished results showed that haptotaxis toward poly-L-lysine was similar for all transfectants indicating no gross differences in the migratory potential of these cells.

Analysis of haptotactic migration by MIP101 carcinoma cells, transfected with the same panel of α^4 mutants, yielded results similar to those obtained with the CHO cells. However, our K562 cell transfectants, and a panel of PMWK melanoma cell transfectants, each showed too little migration activity to be informative.

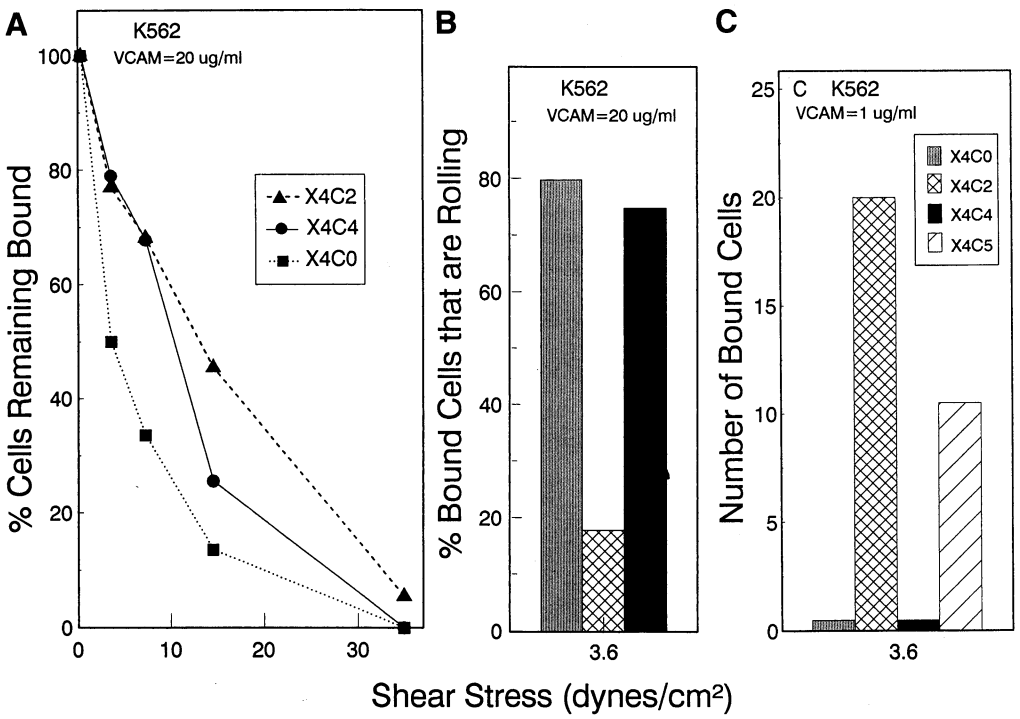

Figure 8. Resistance to shear stress by K562 transfectants on sVCAM-1. (A) K562 cells were allowed to tether to VCAM (20 μg/ml) for 60 s at low shear (0.36 dynes/cm^2). Then, the accumulated cells (100–110 per 0.43 mm^2 field) were subjected to increasing shear stress (in 2–2.5 fold increments at 10 s intervals). After each 10 s interval, the percentage of cells remaining bound (either stationary or rolling) was determined, and these data points are indicated in the line graphs. (B) At a shear stress of 3.6 dynes/cm^2, the percentage of bound cells that were rolling was determined. (C) K562 cells were allowed to tether to low density VCAM (1 μg/ml) for 60 s at low shear (0.36 dynes/cm^2). Then, the accumulated cells (10–20 per 0.43 mm^2 field) were subjected to increasing shear stress (in 2–2.5 fold increments at 10 s intervals). At a shear stress of 3.6 dynes/cm^2, the fraction of cells that remained bound (relative to the initially tethered population) was determined, and is indicated in the bar graph. At higher shear (eg. 15 dynes/cm^2), all of the cells detached.

DISCUSSION

Here we show that the integrin α^4 cytoplasmic domain (compared with α^2 and α^5 tails) supports reduced cell spreading, diminished adhesion strengthening under conditions of shear stress, and impaired localization of the $\alpha^4\beta_1$ integrin into focal adhesion-like complexes formed on an $\alpha^4\beta_1$ ligand (FN40). Conversely, the α^4 tail promoted increased cell migration. Thus, the relatively limited ability of the α^4 tail to engage in strong cytoskeletal interactions may be consistent with the specialized properties of α^4 integrins on highly motile cells such as leukocytes.

We recently showed that $\alpha^4\beta_1$ can mediate cell tethering, continuous rolling, and adhesion strengthening on VCAM-1 under conditions of shear flow (Alon *et al.*, 1995). Notably, the α^4 tail was not needed for initial cell tethering, but did contribute to subsequent adhesion strengthening (Alon *et al.*, 1995). Now we have extended those findings to show that, although the α^4 tail clearly has a positive effect on adhesion strengthening (resistance to detachment), it is relatively weak compared with other cytoplasmic domains ($\alpha^2 > \alpha^5 > \alpha^4$). Thus, as detaching shear stresses were increased, the α^4 tail more readily allowed bound cells to completely detach from the substrate. Furthermore, the α^4 tail also more readily allowed the conversion of stationary adherent K562 cells to rolling cells at higher shear stresses on VCAM-1.

Notably, the integrin α^4, α^2, and α^5 tails all supported initial cell tethering to VCAM or FN40 to a similar extent. This is consistent with the previous finding that deletion of the α^4 tail minimally affected cell tethering under conditions of shear flow (Alon *et al.*, 1995). Taken together, the tethering and adhesion strengthening results indicate that diverse α-chain tails mediate diverse post-ligand binding events, but do not modulate initial ligand interactions required for tethering. Apparently adhesion strengthening is not an important factor in the typical static adhesion assay, as many such assays have failed to reveal consistent differences among the integrin α^2, α^4, and α^5 chain tails (Chan *et al.*, 1992b; Kassner and Hemler, 1993; Kawaguchi and Hemler, 1993; Kassner *et al.*, 1994).

The diminished adhesion strengthening seen with the α^4 tail was paralleled by reduced cell spreading, suggesting that these two events may depend on similar interactions between integrin tails and cytoskeletal proteins. These results are also consistent with a previous finding that the α^2 and α^5 tails, but not the α^4 tail, were able to support integrin-mediated collagen gel contraction (Chan *et al.*, 1992b). Thus, from multiple assays carried out in widely differing cell types, we hypothesize that the α^4 tail yields generally weaker interactions between the integrin and the cytoskeleton.

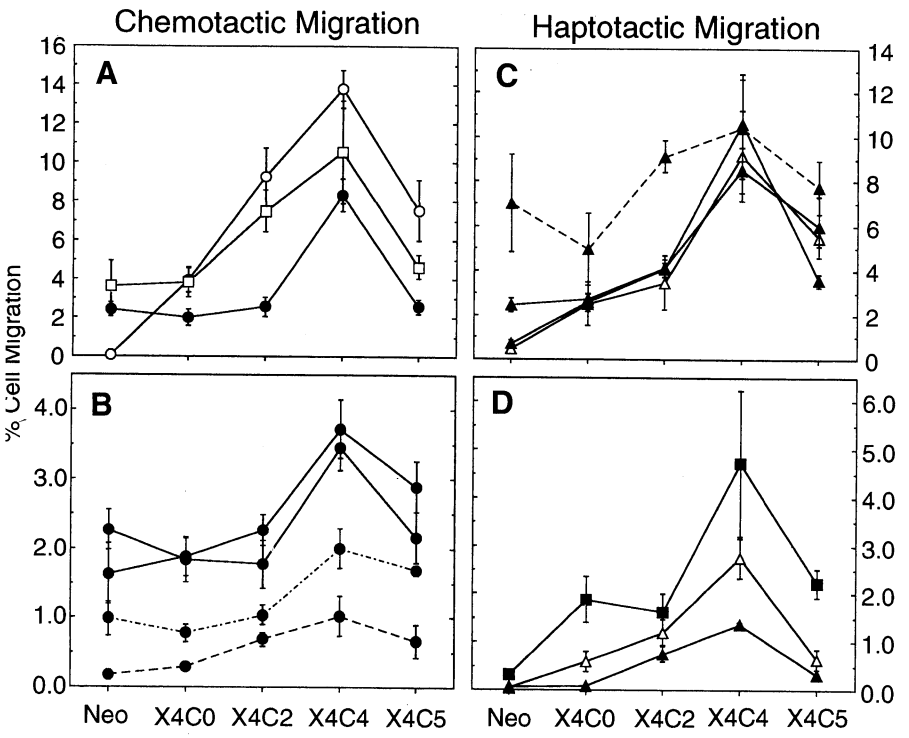

Figure 9. Chemotactic and haptotactic migration of CHO transfectants on FN40. (A and B) For chemotactic migration assays, the percentage of cells migrating through porous filters (coated on both sides with FN40) into a lower well containing 1% FBS, was determined as described in MATERIALS AND METHODS. Results are presented as the mean ± SD for six replicates of a 2-h migration assay. In some experiments (~one-third of the total) little or no migration above the background level was observed, and those results were discarded. (C and D) For haptotactic migration assays (described in MATERIALS AND METHODS), filters were coated with FN40 only on the lower side, and media containing 1% FBS was present on both sides of the filter. Results are presented as the mean ± SD of six replicates of a 4-h migration assay. For chemotactic and haptotactic migration experiments, FN40 coating concentrations were 10 μg/ml (■), 20 μg/ml (△), 25 μg/ml (○), 35 μg/ml (▲), 50 μg/ml (●), and 100 μg/ml (□).

Supporting our hypothesis, the order of adhesion strengthening and cell spreading ($\alpha^2 > \alpha^5 > \alpha^4$) parallels the order of focal adhesion formation ($\alpha^2 > \alpha^5 > \alpha^4$). The decreased ability of α^4 to localize into focal adhesion-like complexes is an obvious manifestation of a reduced ability to interact with focal adhesion components such as α-actinin, vinculin, and talin. Although typical focal adhesion complexes are usually only visible after one or more hours, the types of interactions leading to focal adhesion formation can be observed within minutes (Mueller *et al.*, 1989; Plopper and Ingber, 1993). Now we suggest that some of the same cytoskeletal interactions capable of leading to focal adhesion formation may be functionally obvious even within seconds as tethered cells undergo adhesion strengthening in flow.

Although there is an obvious correlation among the α tails ($\alpha^2 > \alpha^5 > \alpha^4$) with respect to focal adhesion formation, adhesion strengthening, and cell spreading, we must be cautious about over-interpreting α tail deletion (X4C0) results. Despite being deficient in adhesion strengthening and cell spreading, the X4C0 chain was nonetheless able to localize readily into ligand-*de*pendent focal adhesion complexes. Thus, focal adhesions formed in the absence of an α-chain tail may have relatively little functional importance. From α-chain deletion experiments, it was previously concluded that β-chain tail domains are wholly sufficient to organize focal adhesions (LaFlamme *et al.*, 1992; Briesewitz *et al.*, 1993; Ylänne *et al.*, 1993; Kawaguchi *et al.*, 1994). Now we suggest that such focal adhesions are misleading because they have minimal functional relevance. The formation of functionally efficient focal adhesion complexes requires both α and β tails, with the level of function apparently being controlled by the α tail.

Despite observing α tail-dependent differences in the formation of focal adhesion-like structures, we saw no differences in the phosphorylation of $pp125^{FAK}$ (focal adhesion kinase) induced by cross-linking of $\alpha^4\beta_1$ with anti-α^4 mAb. In the CHO cell line, $pp125^{FAK}$ was constitutively phosphorylated (Pasqualini and Hemler, 1994) regardless of antibody induction, and in the K562 cell line, tyrosine phosphorylation of $pp125^{FAK}$ was not detected after cross-linking of any of the chimeras. In another cell line, called MIP101 (Kassner and Hemler, 1993), tyrosine phosphorylation of $pp125^{FAK}$ was induced upon mAb cross-linking, but to the same extent for each chimera. Thus for these cell lines, phosphorylation of $pp125^{FAK}$ was not closely correlated with a differential ability to form focal adhesions. Also, we failed to observe any other consistent differences in the pattern of tyrosine-phosphorylated proteins obtained after triggering the various α^4 transfectants either by mAb or by ligand.

Previously we demonstrated that the α^4 tail surpassed the α^2 or α^5 tails in supporting VLA-2–dependent random cell migration on collagen or laminin-coated surfaces (Chan *et al.*, 1992b). Here we have utilized a different integrin (VLA-4 instead of VLA-2),

different ligand (FN40), a different cell line (CHO), and different types of migration assays (chemotactic and haptotactic migration), to provide additional evidence supporting the pro-migratory role of the α^4 cytoplasmic tail. Apparently, the weaker cytoskeletal interactions and reduced adhesion strengthening mediated by the α^4 tail (compared with α^2 or α^5 tails) make it better suited for transient interactions, such as occur during cell migration (and during rolling under conditions of shear flow). One potential problem with the CHO cell migration studies is that endogenous hamster α^5 could have influenced the hierarchy of results obtained using transfected human α chains, perhaps by selectively altering X4C5 function. However, because a similar hierarchy of cytoplasmic tail effects (C4 > C5 ≈ C2) was seen in a cell line lacking endogenous α^5 (Kassner, unpublished data) this appears not to be an issue. Also in another study, the α^4 tail was compared with the α^3 tail and again was found to promote increased cell migration (Weitzman and Hemler, unpublished data).

An inverse correlation between strength of adhesion and rate of migration has been previously noted. For example, in the CHO cell line the cytoplasmic domain of β_5, compared with β_1, was associated with enhanced migration and reduced focal adhesion formation (Pasqualini and Hemler, 1994). Similarly, when disassembly of focal adhesions was induced in fibroblasts, the cells became more migratory (Dunlevy and Couchman, 1993). However, we should not overextend this inverse correlation, especially because the X4C0 chain showed little capacity to support either adhesion strengthening or migration. Thus, at least a low level of adhesion strengthening appears to be critical for migration. Also, we do not suggest that the α^2 and α^5 integrin subunits cannot mediate migration, only that α^4 has a greater relative ability to support it. Indeed, α^5 and α^2 can participate in integrin-dependent cell migration (Giancotti and Ruoslahti, 1990; Yamada *et al.*, 1990; Grzesiak *et al.*, 1992; Bauer *et al.*, 1993; Leavesley *et al.*, 1993).

In previous studies, α tails have largely been seen as negative regulators, restricting integrin access to inappropriate focal adhesion sites (LaFlamme *et al.*, 1992; Briesewitz *et al.*, 1993; Ylänne *et al.*, 1993; Kawaguchi *et al.*, 1994). Now it is clear that diverse α-chain tails play positive, but variable roles in regulating cell migration, spreading, and strength of adhesion, and that this is paralleled by their capacity to form focal adhesions. The α^4 tail in particular may be well suited to support VLA-4–dependent migration of leukocytes into inflammatory sites (Lobb and Hemler, 1994). In this regard, lymphocytes show VLA-4–dependent migration beneath stromal cells in culture (Miyake *et al.*, 1992) and into brain (Yednock *et al.*, 1992; Baron *et al.*, 1993) and other inflammatory sites (Issekutz, 1991), monocytes utilize VLA-4 for transendothelial migration (Chuluyan and Issekutz, 1993), and Langerhans cells may use VLA-4 for migration from the epidermis into lymph nodes (Aiba *et al.*, 1993). We predict that the specialized properties of the α^4 tail may also make it well suited for its roles in development (Sheppard *et al.*, 1994; Stepp *et al.*, 1994; Yang *et al.*, 1995) and melanoma metastasis (Qian *et al.*, 1994). Whereas most studies thus far have concentrated on the specific extracellular ligand binding properties of α^4, studies of the α^4 tail should now provide another avenue for understanding and ultimately modulating specific VLA-4–mediated functions.

ACKNOWLEDGMENTS

We thank Dr. Roy Lobb (Biogen, Cambridge, MA) for providing recombinant soluble VCAM-1. This work was supported by National Institutes of Health Grants GM-46526 (to M.E.H.), CA-31798, and HL-48675 (to T.A.S.). R.A. is supported by an EMBO fellowship.

REFERENCES

Aiba, S., Nakagawa, S., Ozawa, H., Miyake, K., Yagita, H., and Tagami, H. (1993). Up-regulation of alpha-4 integrin on activated Langerhans cells: analysis of adhesion molecules on Langerhans cells relating to their migration from skin to draining lymph nodes. J. Invest. Derm. *100*, 143–147.

Alon, R., Kassner, P.D., Carr, M.W., Finger, E.B., Hemler, M.E., and Springer, T.A. (1995). The integrin VLA-4 supports tethering and rolling in flow on VCAM-1. J. Cell Biol. *128*, 1243–1253.

Baron, J.L., Madri, J.A., Ruddle, N.H., Hashim, G., and Janeway, C.A. (1993). Surface expression of α4 integrin by CD4 T cells is required for their entry into brain parenchyma. J. Exp. Med. *177*, 57–68.

Bauer, J.S., Varner, J., Schreiner, C., Kornberg, L., Nicholas, R., and Juliano, R.L. (1993). Functional role of the cytoplasmic domain of the integrin α5 subunit. J. Cell Biol. *122*, 209–221.

Berlin, C., Berg, E.L., Briskin, M.J., Andrew, D.P., Kilshaw, P.J., Holzmann, B., Weissman, I.L., Hamann, A., and Butcher, E.C. (1993). α4β7 integrin mediates lymphocyte binding to the mucosal vascular addressin MAdCAM-1. Cell *74*, 185–195.

Briesewitz, R., Kern, A., and Marcantonio, E.E. (1993). Ligand-dependent and -independent integrin focal contact localization: the role of the α chain cytoplasmic domain. Mol. Biol. Cell *4*, 593–604.

Burridge, K., Fath, K., Kelly, T., Nuckolls, G., and Turner, C. (1988). Focal adhesions: transmembrane junctions between the extracellular matrix and the cytoskeleton. Annu. Rev. Cell Biol. *4*, 487–525.

Byers, H.R., Etoh, T., Doherty, J.R., Sober, A.J., and Mihm, M.C., Jr. (1991). Cell migration and actin organization in cultured human primary, recurrent cutaneous and metastatic melanoma. Am. J. Pathol. *139*, 1–13.

Chan, B.M.C., Elices, M.J., Murphy, E., and Hemler, M.E. (1992a). Adhesion to VCAM-1 and fibronectin: comparison of α4β1 (VLA-4) and α4β7 on the human cell line JY. J. Biol. Chem. *267*, 8366–8370.

Chan, B.M.C., Kassner, P.D., Schiro, J.A., Byers, H.R., Kupper, T.S., and Hemler, M.E. (1992b). Distinct cellular functions mediated by different VLA integrin α subunit cytoplasmic domains. Cell *68*, 1051–1060.

Chan, P-Y., and Aruffo, A. (1993). VLA-4 integrin mediates lymphocyte migration on the inducible endothelial cell ligand VCAM-1 and

the extracellular matrix ligand fibronectin. J. Biol. Chem. *268*, 24655–24664.

Chen, Y.-P., O'Toole, T.E., Shipley, T., Forsyth, J., LaFlamme, S.E., Yamada, K.M., Shattil, S.J., and Ginsberg, M.H. (1994). "Inside-out" signal transduction inhibited by isolated integrin cytoplasmic domains. J. Biol. Chem. *269*, 18307–18310.

Chuluyan, H.E., and Issekutz, A.C. (1993). VLA-4 integrin can mediate CD11 CD18-independent transendothelial migration of human monocytes. J. Clin. Invest. *92*, 2768–2777.

Damle, N.K., Klussman, K., Leytze, G., Aruffo, A., Linsley, P.S., and Ledbetter, J.A. (1993). Costimulation with integrin ligands intercellular adhesion molecule-1 or vascular cell adhesion molecule-1 augments activation-induced death of antigen-specific $CD4^+$ T lymphocytes. J. Immunol. *151*, 2368–2379.

Dunlevy, J.R., and Couchman, J.R. (1993). Controlled induction of focal adhesion disassembly and migration in primary fibroblasts. J. Cell Sci. *105*, 489–500.

Elices, M.J., Osborn, L., Takada, Y., Crouse, C., Luhowskyj, S., Hemler, M.E., and Lobb, R.R. (1990). VCAM-1 on activated endothelium interacts with the leukocyte integrin VLA-4 at a site distinct from the VLA-4/fibronectin binding site. Cell *60*, 577–584.

Freedman, A.S., Rhynhart, K., Nojima, Y., Svahn, J., Eliseo, L., Benjamin, C.D., Morimoto, C., and Vivier, E. (1993). Stimulation of protein tyrosine phosphorylation in human B cells after ligation of the β1 integrin VLA-4. J. Immunol. *150*, 1645–1652.

García-Pardo, A., and Ferreira, O.C. (1989). Adhesion of human T-lymphoid cells to fibronectin is mediated by two different fibronectin domains. Immunology *69*, 121–126.

Garcia-Pardo, A., Rostagno, A., and Frangione, B. (1987). Primary structure of human plasma fibronectin: characterization of a 38 kDa domain containing C-terminal heparin-binding site (Hep III site) and a region of molecular heterogeneity. Biochem. J. *241*, 923–928.

Giancotti, F.G., and Ruoslahti, E. (1990). Elevated levels of the $\alpha^5\beta_1$ fibronectin receptor suppress the transformed phenotype of Chinese hamster ovary cells. Cell *60*, 849–859.

Grzesiak, J.J., Davis, G.E., Kirchhofer, D., and Pierschbacher, M.D. (1992). Regulation of $\alpha_2\beta_1$-mediated fibroblast migration on type I collagen by shifts in the concentrations of extracellular Mg^{2+} and Ca^{2+}. J. Cell Biol. *117*, 1109–1117.

Guan, J-L., and Hynes, R.O. (1990). Lymphoid cells recognize an alternatively spliced segment of fibronectin via the integrin receptor $\alpha4\beta1$. Cell *60*, 53–61.

Hemler, M.E., Huang, C., Takada, Y., Schwarz, L., Strominger, J.L., and Clabby, M.L. (1987). Characterization of the cell surface heterodimer VLA-4 and related peptides. J. Biol. Chem. *262*, 11478–11485.

Hemler, M.E., and Strominger, J.L. (1982). Monoclonal antibodies reacting with immunogenic mycoplasma proteins present in human hematopoietic cell lines. J. Immunol. *129*, 2734–2738.

Hemler, M.E., Weitzman, J.B., Pasqualini, R., Kawaguchi, S., Kassner, P.D., and Berdichevsky, F.B. (1994). Structure, biochemical properties, and biological functions of integrin cytoplasmic domains, In: Integrin: The Biological Problem, ed. Y. Takada, Ann Arbor, MI: CRC Press, 1–35.

Issekutz, T.B. (1991). Inhibition of in vivo lymphocyte migration to inflammation and homing to lymphoid tissues by the TA-2 monoclonal antibody. J. Immunol. *147*, 4178–4184.

Kassner, P.D., and Hemler, M.E. (1993). Interchangeable alpha chain cytoplasmic domains play a positive role in control of cell adhesion mediated by VLA-4, a β_1-integrin. J. Exp. Med. *178*, 649–660.

Kassner, P.D., Kawaguchi, S., and Hemler, M.E. (1994). Minimum α chain sequence needed to support integrin-mediated adhesion. J. Biol. Chem. *269*, 19859–19867.

Kawaguchi, S., Bergelson, J.M., Finberg, R.W., and Hemler, M.E. (1994). Integrin α^2 cytoplasmic domain deletion effects: loss of adhesive activity parallels ligand-independent recruitment into focal adhesions. Mol. Biol. Cell *5*, 977–988.

Kawaguchi, S., and Hemler, M.E. (1993). Role of the α subunit cytoplasmic domain in regulation of adhesive activity mediated by the integrin VLA-2. J. Biol. Chem. *268*, 16279–16285.

Koopman, G., Keehnen, R.M.J., Lindhout, E., Newman, W., Shimizu, Y., Van Seventer, G.A., de Groot, C., and Pals, S.T. (1994). Adhesion through the LFA-1 (CD11a/CD18)-ICAM-1 (CD54) and the VLA-4 (CD49d)-VCAM-1 (CD106) pathways prevents apoptosis of germinal center B cells. J. Immunol. *152*, 3760–3767.

LaFlamme, S.E., Akiyama, S.K., and Yamada, K.M. (1992). Regulation of fibronectin receptor distribution. J. Cell Biol. *117*, 437–447.

LaFlamme, S.E., Thomas, L.A., Yamada, S.S., and Yamada, K.M. (1994). Single subunit chimeric integrins as mimics and inhibitors of endogenous integrin functions in receptor localization, cell spreading and migration, and matrix assembly. J. Cell Biol. *126*, 1287–1298.

Lawrence, M.B., and Springer, T.A. (1991). Leukocytes roll on a selectin at physiologic flow rates: distinction from and prerequisite for adhesion through integrins. Cell *65*, 859–873.

Leavesley, D.I., Schwartz, M.A., Rosenfeld, M., and Cheresh, D.A. (1993). Integrin $\beta1$- and $\beta3$-mediated endothelial cell migration is triggered through distinct signalling mechanisms. J. Cell Biol. *121*, 163–170.

Lobb, R.R., Chi-Rosso, G., Leone, D.R., Rosa, M.D., Newman, B.M., Luhowskyj, S., Osborn, L., Schiffer, S.G., Benjamin, C.D., Dougas, I.G., Hession, C., and Chow, E.P. (1991). Expression and functional characterization of a soluble form of vascular cell adhesion molecule 1 (VCAM1). Biochem. Biophys. Res. Commun. *178*, 1498–1504.

Lobb, R.R., and Hemler, M.E. (1994). The pathophysiologic role of $\alpha4$ integrins in vivo. J. Clin. Invest. *269*, 8348–8354.

Lukashev, M.E., Sheppard, D., and Pytela, R. (1994). Disruption of integrin function and induction of tyrosine phosphorylation by the autonomously expressed β_1 integrin cytoplasmic domain. J. Biol. Chem. *269*, 18311–18314.

Marcantonio, E.E., Guan, J., Trevithick, J.E., and Hynes, R.O. (1990). Mapping of the functional determinants of the integrin beta-1 cytoplasmic domain by site-directed mutagenesis. Cell Regul. *1*, 597–604.

Miyake, K., Hasunuma, Y., Yagita, H., and Kimoto, M. (1992). Requirement for VLA-4 and VLA-5 integrins in lymphoma cells binding to and migration beneath stromal cells in culture. J. Cell Biol. *119*, 653–662.

Mueller, S.C., Kelly, T., Dai, M., Dai, H., and Chen, W.-T. (1989). Dynamic cytoskeleton-integrin associations induced by cell binding to immobilized fibronectin. J. Cell Biol. *109*, 3455–3464.

Nojima, Y., Rothstein, D.M., Sugita, K., Schlossman, S.F., and Morimoto, C. (1992). Ligation of VLA-4 on T cells stimulates tyrosine phosphorylation of a 105-kD protein. J. Exp. Med. *175*, 1045–1053.

O'Toole, T.E., Katagiri, Y., Faull, R.J., Peter, K., Tamura, R.N., Quaranta, V., Loftus, J.C., Shattil, S.J., and Ginsberg, M.H. (1994). Integrin cytoplasmic domains mediate inside-out signal transduction. J. Cell Biol. *124*, 1047–1059.

O'Toole, T.E., Mandelman, D., Forsyth, J., Shattil, S.J., Plow, E.F., and Ginsberg, M.H. (1991). Modulation of the affinity of integrin $\alpha IIb\beta3$ (GPIIb-IIIa) by the cytoplasmic domain of αIIb. Science *254*, 845–847.

Papayannopoulou, T., and Nakamoto, B. (1993). Peripheralization of hemopoietic progenitors in primates treated with anti-VLA4 integrin. Proc. Natl. Acad. Sci. USA *90*, 9374–9378.

Pasqualini, R., and Hemler, M.E. (1994). Contrasting roles for integrin $\beta 1$ and $\beta 5$ cytoplasmic domains in subcellular localization, cell proliferation, and cell migration. J. Cell Biol. *125*, 447–460.

Plopper, G., and Ingber, D.E. (1993). Rapid induction and isolation of focal adhesion complexes. Biochem. Biophys. Res. Commun. *193*, 571–578.

Qian, F., Vaux, D.L., and Weissman, I.L. (1994). Expression of the integrin $\alpha 4\beta 1$ on melanoma cells can inhibit the invasive stage of metastasis formation. Cell *77*, 335–347.

Reszka, A.A., Hayashi, Y., and Horwitz, A.F. (1992). Identification of amino acid sequences in the integrin β_1 cytoplasmic domain implicated in cytoskeletal association. J. Cell Biol. *117*, 1321–1330.

Rice, G.E., and Bevilacqua, M.P. (1989). An inducible endothelial cell surface glycoprotein mediates melanoma adhesion. Science *246*, 1303–1306.

Rice, G.E., Munro, J.M., and Bevilacqua, M.P. (1990). Inducible cell adhesion molecule 110 (INCAM-110) is an endothelial receptor for lymphocytes: a CD11/CD18-independent adhesion mechanism. J. Exp. Med. *171*, 1369–1374.

Romanic, A.M., and Madri, J.A. (1994). The induction of 72-kD gelatinase in T cells upon adhesion to endothelial cells is VCAM-1 dependent. J. Cell Biol. *125*, 1165–1178.

Rosen, G.D., Sanes, J.R., LaChance, R., Cunningham, J.M., Roman, J., and Dean, D.C. (1992). Roles for the integrin VLA-4 and its counter receptor VCAM-1 in myogenesis. Cell *69*, 1107–1119.

Rüegg, C., Postigo, A., Sikorski, E.E., Butcher, E.C., Pytela, R., and Erle, D.J. (1992). Role of integrin $\alpha 4\beta 7/\alpha 4\beta P$ in lymphocyte adherence to fibronectin and VCAM-1 and in homotypic cell clustering. J. Cell Biol. *117*, 179–189.

Sastry, S.K., and Horwitz, A.F. (1993). Integrin cytoplasmic domains: mediators of cytoskeletal linkages and extra- and intracellular initiated transmembrane signaling. Curr. Opin. Cell Biol. *5*, 819–831.

Sánchez-Madrid, F., De Landazuri, M.O., Morago, G., Cebrian, M., Acevedo, A., and Bernabeu, C. (1986). VLA-3: a novel polypeptide association within the VLA molecular complex. Cell distribution and biochemical characterization. Eur. J. Immunol. *16*, 1343–1349.

Schreiner, C.L., Bauer, J.S., Danilov, Y.N., Hussein, S., Sczekan, M.M., and Juliano, R.L. (1989). Isolation and characterization of Chinese hamster ovary cell variants deficient in the expression of fibronectin receptor. J. Cell Biol. *109*, 3157–3167.

Schwartz, B.R., Wayner, E.A., Carlos, T.M., Ochs, H.D., and Harlan, J.M. (1990). Identification of surface proteins mediating adherence of CD11/CD18-deficient lymphoblastoid cells to cultured human endothelium. J. Clin. Invest. *85*, 2019–2022.

Sheppard, A.M., Onken, M.D., Rosen, G.D., Noakes, P.G., and Dean, D.C. (1994). Expanding roles for $\alpha 4$ integrin and its ligands in development. Cell Adhes. Comm. *2*, 27–43.

Smilenov, L., Briesewitz, R., and Marcantonio, E.E. (1994). Integrin $\beta 1$ cytoplasmic domain dominant negative effects revealed by lysophosphatidic acid treatment. Mol. Biol. Cell *5*, 1215–1223.

Stepp, M.A., Urry, L.A., and Hynes, R.O. (1994). Expression of $\alpha 4$ integrin mRNA and protein and fibronectin in the early chicken embryo. Cell Adhes. Comm. *2*, 359–375.

Wayner, E.A., García-Pardo, A., Humphries, M.J., McDonald, J.A., and Carter, W.G. (1989). Identification and characterization of the lymphocyte adhesion receptor for an alternative cell attachment domain in plasma fibronectin. J. Cell Biol. *109*, 1321–1330.

Williams, D.A., Rios, M., Stephens, C., and Patel, V.P. (1991). Fibronectin and VLA-4 in haematopoietic stem cell-microenvironment interactions. Nature *352*, 438–441.

Woods, A., McCarthy, J.B., Furcht, L.T., and Couchman, J.R. (1993). A synthetic peptide from the COOH-terminal heparin-binding domain of fibronectin promotes focal adhesion formation. Mol. Biol. Cell *4*, 605–613.

Yamada, K.M., Kennedy, D.W., Yamada, S.S., Gralnick, H., Chen, W.-T., and Akiyama, S.K. (1990). Monoclonal antibody and synthetic peptide inhibitors of human tumor cell migration. Cancer Res. *50*, 4485–4496.

Yang, J.T., Rayburn, H., and Hynes, R.O. (1995). Cell adhesion events mediated by $\alpha 4$ integrins are essential in placental and cardiac development. Development *(in press)*.

Yednock, T.A., Cannon, C., Fritz, L.C., Sánchez-Madrid, F., Steinman, L., and Karin, N. (1992). Prevention of experimental autoimmune encephalomyelitis by antibodies against $\alpha 4\beta 1$ integrin. Nature *356*, 63–66.

Ylänne, J., Chen, Y., O'Toole, T.E., Loftus, J.C., Takada, Y., and Ginsberg, M.H. (1993). Distinct functions of integrin α and β subunit cytoplasmic domains in cell spreading and formation of focal adhesions. J. Cell Biol. *122*, 223–233.

Yurochko, A.D., Liu, D.Y., Eierman, D., and Haskill, S. (1992). Integrins as a primary signal transduction molecule regulating monocyte immediate-early gene induction. Proc. Natl. Acad. Sci. USA *89*, 9034–9038.